Research Article | Vol. 26, No. 6 | 19 Mar 2018 | OPTICS EXPRESS 7098
Optics EXPRESS

Control of the coherence behavior in a SFG interferometer through the multipump phases command

P. DARRÉ,[1,2] L. LEHMANN,[1] L. GROSSARD,[1] L. DELAGE,[1] AND F. REYNAUD[1,*]

[1] *Univ. Limoges, CNRS, XLIM, UMR 7252, F-87000 Limoges, France*
[2] *Current address: European Southern Observatory, Karl-Schwarzschild-Str. 2, Garching bei München 85748, Germany*
[*] *francois.reynaud@unilim.fr*

Abstract: In this paper, we report on a novel method to control the coherence behavior in a sum frequency generation interferometer powered by two independent pump lines. At the output of the interferometer, the two incoherent fringe patterns must be superimposed to maximize the contrast. The first step consists in canceling the differential group delay. The second one uses the phase control on one pump to synchronize the fringe patterns. This innovative method is experimentally demonstrated with a setup involving a 1544 nm signal and two pump lines around 1064 nm leading to a converted signal around 630 nm. It can be easily extended to a greater number of pump lines.

OCIS codes: (030.1640) Coherence; (120.2650) Fringe analysis; (120.3180) Interferometry; (160.3730) Lithium niobate; (190.7220) Upconversion; (230.7370) Waveguides.

References and links

1. C. Langrock, E. Diamanti, R. V. Roussev, Y. Yamamoto, and M. M. Fejer, "Highly efficient single-photon detection at communication wavelengths by use of upconversion in reverse-proton-exchanged periodically poled $LiNbO_3$ waveguides," Opt. Lett. **30**(13), 1725–1727 (2005).
2. H. Xia, G. Shentu, M. Shangguan, X. Xia, X. Jia, C. Wang, J. Zhang, J. S. Pelc, M. M. Fejer, Q. Zhang, X. Dou, and J. W. Pan, "Long-range micro-pulse aerosol lidar at 1.5μm with an upconversion single-photon detector," Opt. Lett. **40**(7), 1579–1582 (2015).
3. A. Barh, C. Pedersen, and P. Tidemand-Lichtenberg, "Ultra-broadband mid-wave-IR upconversion detection," Opt. Lett. **42**(8), 1504–1507 (2017).
4. Q. Zhang, C. Langrock, M. M. Fejer, and Y. Yamamoto, "Waveguide-based single pixel up-conversion infrared spectrometer," Opt. Express **16**(24), 19557–19561 (2008).
5. Y.-H. Cheng , T. Thomay, G. S. Solomon , A. L. Migdall, S. V. Polyakov, "Statistically background-free, phase-preserving parametric up-conversion with faint light," Opt. Express **23**(14), 18671–18678 (2015).
6. F. Marsili, V. B. Verma, J. A. Stern, S. Harrington, A. E. Lita, T. Gerrits, I. Vayshenker, B. Baek, M. D. Shaw, R. P. Mirin, and S. W. Nam, "Detecting single infrared photons with 93 % system efficiency," Nature Photonics **7**(3), 210–214 (2013).
7. M. Asobe, O. Tadanaga, H. Miyazawa, Y. Nishida, and H. Suzuki, "Multiple quasi-phase-matched device using continuous phase modulation of $\chi^{(2)}$ grating and its application to variable wavelength conversion," IEEE J. Quantum Electron. **41**(12), 1540–1547, (2005).
8. R. T. Thew, H. Zbinden, and N. Gisin, "Tunable upconversion photon detector," Appl. Phys. Lett. **93**, 071104 (2008).
9. P. Darré, R. Baudoin, J.-T. Gomes, N. J. Scott, L. Delage, L. Grossard, J. Sturmann, C. Farrington, F. Reynaud, and T. A. Ten Brummelaar, "First On-Sky Fringes with an Up-Conversion Interferometer Tested on a Telescope Array," Phys. Rev. Lett. **117**, 233902 (2016).
10. L. Szemendera, P. Darré, R. Baudoin, L. Grossard, L. Delage, H. Herrmann, C. Silberhorn, F. Reynaud, "In-lab ALOHA mid-infrared up-conversion interferometer with high fringe contrast @λ = 3.39μm," Monthly Notices of the Royal Astronomical Society **457**(3), 3115–3118, (2016).
11. J.-T. Gomes, L. Grossard, D. Ceus, S. Vergnole, L. Delage, F. Reynaud, H. Herrmann, and W. Sohler, "Demonstration of a frequency spectral compression effect through an up-conversion interferometer," Opt. Express **21**(3), 3073–3082 (2013).
12. P. Darré, L. Szemendera, L. Grossard, L. Delage and F. Reynaud, "Effect of spectral sampling on the temporal coherence analysis of a broadband source in a SFG interferometer," Opt. Express **23**(20), 25450–25461 (2015).

#318209 https://doi.org/10.1364/OE.26.007098
Journal © 2018 Received 21 Dec 2017; revised 8 Feb 2018; accepted 12 Feb 2018; published 8 Mar 2018

Optics EXPRESS

13. S. Kurimura, Y. Kato, M. Maruyama, Y. Usui, H. Nakajima, "Quasi-phase-matched adhered ridge waveguide in LiNb O3," Appl. Phys. Lett. **89**, 191123 (2006).
14. R. W. Boyd, *Nonlinear Optics* (Academic, 2008).

1. Introduction

Sum frequency generation (SFG) using periodically poled Lithium Niobate (PPLN) crystals becomes a useful tool for a large number of applications in the optical domains such as infrared detection in the photon counting regime [1,2], spectroscopy [3,4] and quantum applications [5,6]. All over these applications, implemented with a monochromatic pump, the experimental results are driven by a trade-off between the spectral bandwidth and the conversion efficiency [7,8].

For more than a decade we investigate a new concept of fiber interferometer involving a non-linear stage in each arm: the SFG interferometer. The main purpose of this research activity consists of an alternative technique for high resolution imaging with telescope array in the near and mid-infrared spectral domains [9,10]. To broaden the converted infrared spectrum of the instrument, we have proposed the use of a multispectral pump. In previous studies [11,12], we demonstrated the possibility to simultaneously process two infrared samples with two independent laser pumps in each of the two PPLN of the SFG interferometer, and showed original properties of the coherence behavior such as frequency spectral compression effect. When converting a broadband infrared signal spectrum with a dual pump powering the non-linear stage in each arm of a SFG interferometer, two fringe patterns are independently generated and must be superimposed to optimize the sensibility of the instrument.

As usual, the fringe patterns are centered on the acquisition window by actuating a delay line to cancel the differential group delay, which constitutes the first parameter to control. Then, when the group delay is set to zero, the fringe patterns must be actively synchronized to efficiently build up the contributions of each spectral channel. The second parameter is the relative phases between the fringe patterns contributing to the global interferometric signal and must be adjusted precisely. With only two pump lines, the synchronization of the fringe patterns can hardly be achieved through a complex iterative process using two delay lines implemented on the signal and converted paths. Expanding the two-pump configuration to N pumps leads to the generation of N fringe patterns related to each pump line. Here again, the group delay has to be first set to zero. When implemented with more than two pump lines, the contrast has to be managed by the simultaneous synchronization of all the fringe patterns leading to control N-1 parameters. This cannot be achieved only with the delay lines and makes necessary to propose a new configuration with more degrees of freedom.

In this paper, we propose an original valuable configuration for synchronization of the fringe patterns in order to set the interferometer at the maximum of contrast in a multipump configuration. For this purpose, we describe an active method to manage the differential spectral phase of the converted fields through a control of the differential phase of the pump fields. For the sake of simplicity and cost considerations, the experimental demonstration is achieved with two pump lines, but could be easily extended to more pump lines.

2. General description of the upconversion interferometer

The experimental setup given in Fig. 1 is based on a Mach-Zehnder interferometer using guided and polarization maintaining single mode optical components. All the lengths of the optical arms are equalized to within a few millimeters. We passively insure a thermal and mechanical isolation of the instrument in order to cancel any significant phase fluctuations during the different measurements. A superluminescent diode (SLED) emitting an infrared signal centered at 1544.0 nm with a 40 nm bandwidth feeds the system, and provides an incoherent source and a high flux level (a few mW). Both arms of the interferometer include a sum frequency generation

Optics EXPRESS

process, upconverting the infrared input signal to the visible domain. In the framework of our experiment, the SFG processes take place in periodically poled $LiNbO_3$ waveguides based on a ridge technology [13] and provided by NTT Corporation. The specified conversion efficiencies of these components are better than 150 %/W of pump. The waveguides are 22-mm long and pigtailed with fibers at the input and the output of the device, improving the reliability and the efficiency of the light coupling.

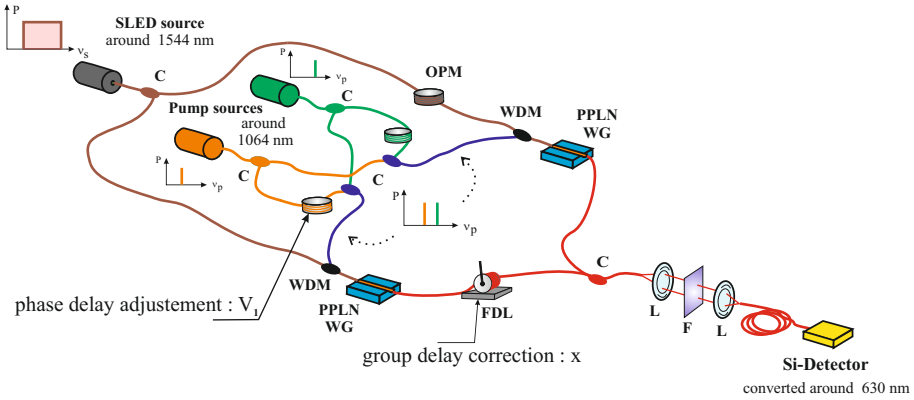

Fig. 1. Experimental setup. OPM: optical path modulator, FDL: fiber delay line, C: 50/50 coupler, WDM: wavelength division multiplexing, WG: waveguide, F: filters, L: lens.

The pump power is provided by a set of two monochromatic mutually incoherent laser lines and emitting at two wavelengths separated by 1.4 nm around 1064.0 nm. The coherence length of each pump line is much greater than the optical path differences on the pump stage. The pumps are equally shared between the two interferometric arms thanks to a fiber coupler to provide the energy required by the SFG process, and to preserve the mutual coherence between the two upconverted waves. The total pump power injected on each of the two PPLN is close to 10 mW. For each pump line and its corresponding converted signal field, the energy conservation through the SFG process implies to fulfill the following relationship:

$$\nu_s + \nu_p = \nu_c, \tag{1}$$

with ν_s, ν_p and ν_c the frequencies of the infrared input signal, the pump and the converted optical signal respectively.

Due to the quasiphase matching condition, the SFG process related to one pump line is only efficient over a narrow infrared spectral range $\Delta\nu_{acc}$ defined as the spectral acceptance, and therefore the non-linear process acts as a frequency filter. In our experiment, the width of the spectral acceptance of each PPLN is close to 0.6 nm around 1544 nm. To ensure the quasiphase matching condition and achieve simultaneously the same expected SFG process on each arm of the instrument, each PPLN is thermally regulated around 54 °C with an accuracy better than 0.1 °C.

Theoretically, the normalized profile $B(\nu)$ of this frequency filtering function can be given by the following expression [14]:

$$B(\nu) = \mathrm{sinc}^2\left(\frac{\nu}{\Delta\nu_{acc}}\right). \tag{2}$$

When using a single line pump at ν_{pi} (i = 1 or 2), the infrared spectrum $B_{si}(\nu_s)$ centered around the frequency ν_{si} upconverted by the non-linear process is simply shifted to the visible spectral domain $B_{ci}(\nu_c)$ around the frequency ν_{ci} without any shape modification (i.e. the spectral

acceptance $\Delta\nu_{acc}$ is then fully preserved).

$$B_{si}(\nu_s) = B(\nu_s - \nu_{si}), \tag{3}$$

and

$$B_{ci}(\nu_c) = B(\nu_c - \nu_{ci}). \tag{4}$$

At the output of the upconversion interferometer, the two converted optical fields are combined through a single mode and polarization maintaining fiber coupler. When simultaneously switching on the two independent pump lines to power the non-linear crystals, two spectral samples centered on the frequencies ν_{s1} and ν_{s2} are simultaneously converted in each PPLN. Figure 2 shows that the converted frequency spectrum exhibits two flipped spectral samples with respect to the infrared spectrum and a compression of the spacing between them, as previously reported in [11, 12].

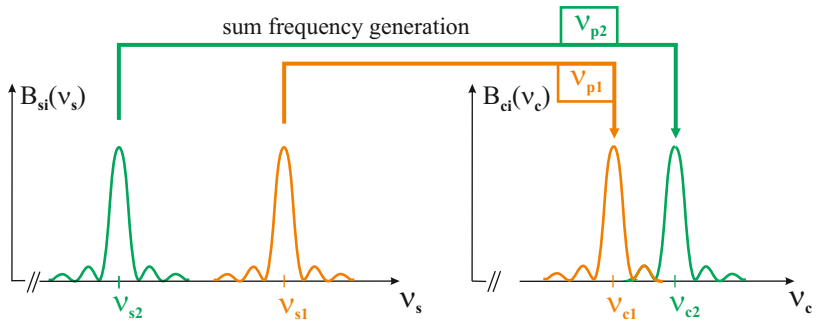

Fig. 2. Power spectral density transfer through the non-linear SFG process when two pump lines converts two different spectral samples centered on the infrared signal frequencies ν_{si}.

In the dual line pump configuration, two independent fringe patterns are observed and must be locally superimposed to achieve high contrast. For this purpose, two phase control functions must be integrated. Firstly, a fiber delay line with 12 cm stroke implemented on one interferometric arm allows us to vary the group delay as a function of the mechanical actuator position x. Secondly, a phase modulator is implemented on each pump path before recombining the two laser lines. These phase modulators are driven by constant voltages V_i to allow the generation of an adjustable differential phase Φ_{pi} for each pump line i . Then, the two pump lines are merged with the infrared signal through a wavelength-division multiplexer (WDM) on each arm of the interferometer in order to feed the SFG stage.

In addition, the infrared stage includes an optical path modulator with a 30 µm stroke on one arm to display the fringes as a function of time. This allows us to measure the fringe contrast around 630 nm with a silicon detector preceded by a set of two bandpass spectral filters with a 40 nm and 2 nm bandwidth, selecting only the converted signal with a 40 nm and 2 nm bandwidth around 630 nm.

3. Differential spectral phase and derivation of the fringe contrast

The analysis of the coherence behavior in the SFG interferometer requires an assessment of the differential spectral phase between the two interferometric arms, due to path length differences in one hand, and differential chromatic dispersion in the other hand. All over the SFG interferometer, the global differential spectral phase related to the pump i, and denoted Φ_i, is the sum of the contributions accumulated in the three stages and can be written as follows:

$$\Phi_i = \Phi_{si}(\nu_s) + \Phi_{pi}(\nu_{pi}) + \Phi_{ci}(\nu_c), \tag{5}$$

Optics EXPRESS

with Φ_{si} the contribution of the infrared stage, Φ_{pi} the phase shift induced on the pump stage and Φ_{ci} the differential spectral phase associated to converted optical fields. Due to Eq. (1) and assuming that the pumps are monochromatic, Φ_i can be expressed as a parametric function of the ν_c variable and the ν_{pi} parameter.

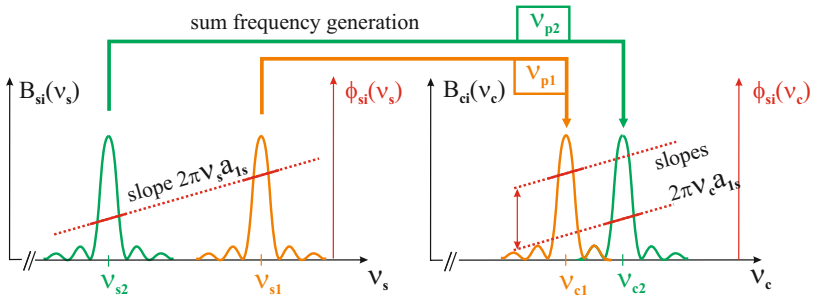

Fig. 3. Spectral phase transfer of the infrared signal through the non-linear process. The spectral compression leads to a discontinuity of the spectral phase when expressed as a function of ν_c.

In our experimental context, the SFG filtering due to the quasiphase matching results in very narrow spectral bandwidths that will be upconverted. The Taylor expansion can therefore be limited to the first-order. Moreover, the two spectral samples are close enough (in the range of few nm) to consider the first-order coefficients a_1 independent of the spectral sample index i in the signal and converted optical field domains.

In the infrared stage, the phase expansion only depends on non adjustable parameters:

$$\Phi_{si} = a_{0si} + a_{1s} \times (\nu_s - \nu_{si}). \tag{6}$$

According to Eq. (1), Φ_{si} can be expressed as a function of ν_c:

$$\Phi_{si} = a_{0si} + a_{1s} \times (\nu_c - \nu_{ci}), \tag{7}$$

where ν_{si} and ν_{ci} correspond to the mean frequency of the signal and converted spectrum with the pump at ν_{pi}. a_{0si} correspond to the zeroth-order coefficients of the differential spectral phase associated to the infrared signal converted by the pump i.

As reported on the right of Fig. 3, the spectral compression induces a discontinuity in the spectral phase of the converted field. Nevertheless, we note that the phase slope a_{1s} related to the infrared samples is preserved by the SFG processes and is the same for the two converted spectral samples.

As the pump lasers are monochromatic, the Φ_{pi} terms are constant and will be experimentally controlled in the pump stage by piezoelectric actuators driven by DC voltages V_i.

$$\Phi_{pi} = K_i V_i, \tag{8}$$

where K_i is a constant in rad/V.

At last, in the visible stage, the phase contribution Φ_{ci} contains a variable term stemming from the fiber delay line actuator position x, and a static term resulting from the differential chromatic dispersion and fiber length differences. It can be written as:

$$\Phi_{ci} = a_{0ci} + k_{0i} x + (a_{1c} + k_1 x) \times (\nu_c - \nu_{ci}), \tag{9}$$

were k_{0i} and k_1 are the zeroth- and first-order coefficients of the fiber delay line differential dispersion function. Table 1 summarizes the different contributions to the spectral phase. The Taylor coefficients a_{0ti} and a_{1t} correspond to the global propagation over the three stages.

Optics EXPRESS

Table 1. General overview of the different spectral phase contributions

order / stage	Zeroth-order	First-order
infrared	a_{0si}	$a_{1s} \times (\nu_s - \nu_{si})$ $a_{1s} \times (\nu_c - \nu_{ci})$
pump	$K_i V_i$	none
visible	$a_{0ci} + k_{0i} x$	$(a_{1c} + k_1 x) \times (\nu_c - \nu_{ci})$
total	$a_{0ti}(x, V_i)$ $= a_{0si} + K_i V_i + a_{0ci} + k_{0i} x$	$a_{1t}(x) \times (\nu_c - \nu_{ci})$ $= (a_{1s} + a_{1c} + k_1 x) \times (\nu_c - \nu_{ci})$

The total differential spectral phase can be synthesized in the formula :

$$\Phi_i = a_{0ti}(x, V_i) + a_{1t}(x) \times (\nu_c - \nu_{ci}). \tag{10}$$

The first-order term a_{1t}, is related to the differential group delay $\tau_g(x)$ between the two arms.

$$a_{1t}(x) = 2\pi\tau_g(x). \tag{11}$$

Due to the first-order approximation on the Taylor expansion of the spectral phase, this differential group delay is identical for the two spectral channels. It can be adjusted by conveniently actuating the fiber delay line position x.

The zeroth-order term a_{0ti} of the Taylor expansion is related to the phase delay. It can be controlled only through the V_i driving voltages of the piezoelectric actuators if x is kept constant.

The knowledge of the power spectral density and the spectral phase allows us to derive the interferometric signal resulting from the incoherent superposition of the fringe patterns each associated with a converted spectral sample i.

$$I(x, V_1, V_2) = \sum_{i=1}^{N=2} \Re\left(\int B \times (\nu_c - \nu_{ci}) \left\{ 1 + \exp\left[j2\pi\tau_g \times (\nu_c - \nu_{ci}) \right] \exp\left[j a_{0ti}(x, V_i) \right] \right\} d\nu_c \right). \tag{12}$$

Thus, the fringe contrast can be expressed as a function of the delay line position x and the piezoelectric voltages V_i as following:

$$C(x, V_1, V_2) = \text{Triangle}\left(\frac{\Delta\nu_{acc}\tau_g(x)}{\pi} \right) \left| \cos\left(\frac{a_{0t2}(x, V_2) - a_{0t1}(x, V_1)}{2} \right) \right|. \tag{13}$$

4. Principle and experimental demonstration of the phase control in a SFG interferometer analyzing a broadband infrared source

The coherence properties of the converted fields can be controlled through the delay line position implemented on the visible stage, and the phase modulators implemented on the pump stage. It is thus possible to optimize the fringe contrast in two independent steps.

In a first step, the differential group delay term $\tau_g(x)$ (i.e. the first-order term of the Taylor expansion) is canceled to maximize the triangle function in the contrast expression.

$$\tau_g(x_0) = 0 \rightarrow \text{Triangle}\left(\frac{\Delta\nu_{acc}\tau_g(x_0)}{\pi} \right) = 1. \tag{14}$$

As a consequence, the two triangular contrast envelops related to each fringe system are centered in the acquisition window and perfectly overlapped, as shown in Fig. 4.

Optics EXPRESS

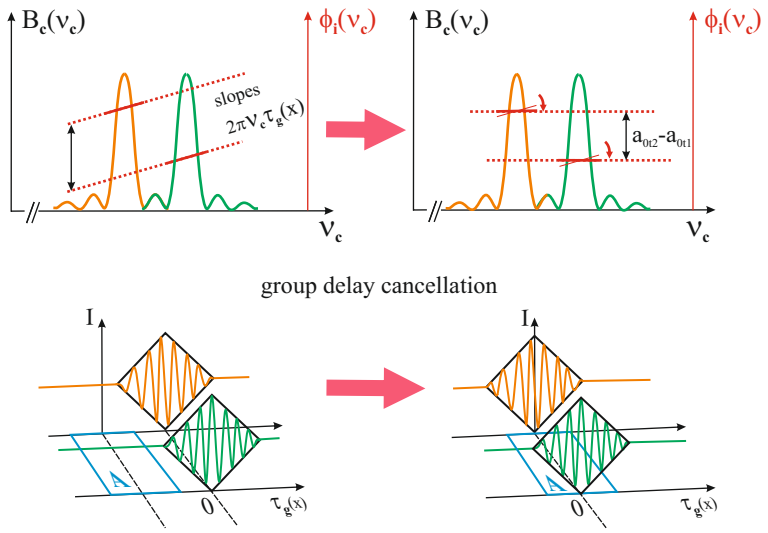

Fig. 4. Synchronized envelopes without fringe pattern synchronization. A: fringe acquisition window.

In a second step, the zeroth-order terms of the Taylor expansion have to be set to zero modulo 2π to maximize the absolute value of the cosine function (Fig. 5).

$$\left|\cos\left(\frac{a_{0t2}\left(x_0, V_2\right) - a_{0t1}\left(x_0, V_1\right)}{2}\right)\right| = 1. \tag{15}$$

This implies to adjust the driving voltages V_i without modification of x_0 so that:

$$a_{0t2}\left(x_0, V_2\right) - a_{0t1}\left(x_0, V_1\right) = 0 \text{ modulo } 2\pi. \tag{16}$$

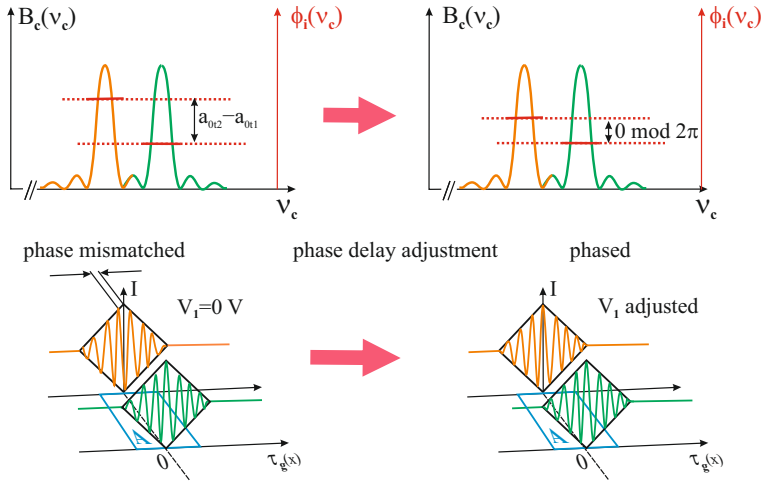

Fig. 5. Synchronized envelopes with fringe pattern synchronization.

Note that this synchronization procedure of the fringe patterns can be easily extended to any number N of pump lines. The differential group delays of the fringe patterns are first cancelled with the delay line on the visible stage (all at once). Then the fringe patterns are superimposed by adjusting N-1 independent voltages, each controlling the corresponding zeroth-order term of the Taylor expansion.

Optics EXPRESS

In our two-pump line experiment, the differential group delay term $\tau_g(x)$ is first cancelled by adjusting the delay line position x on the visible stage at the specific position x_0. Then, we measure the contrast for different shifts between the two fringe patterns. Each shift is set using the phase modulator implemented on one pump path, driven by a constant voltage V_1 to create a differential pump phase. The voltage V_2 is set to 0 V. It should be noted that, for fixed values of x and V_1, the stability of the optical path difference has been observed for a period greater than one hour.

Figure 6 represents the experimental fringe contrasts for different driving voltages V_1. We experimentally retrieve the evolution of the fringe contrast as an absolute value of a cosine term as theoretically predicted in Eq. (13), assuming $\tau_g(x_0) = 0$. According to the experimental results, two contiguous maximums of contrast are separated by an offset command of 320 mV corresponding to a 2π shift of the differential pump phase Φ_p.

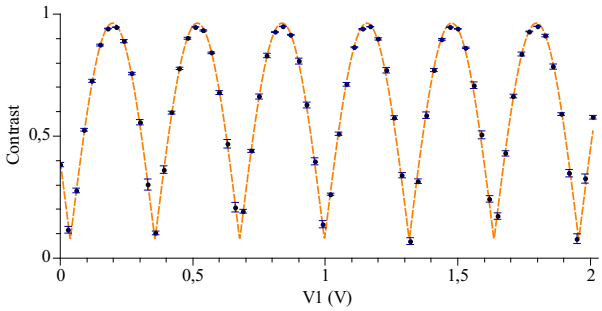

Fig. 6. Measured contrast as a function of the voltage V_1 applied on the phase modulator integrated on one optical path linked to the pump source. This contrast evolution is obtained after canceling the differential group delay τ_g. The dashed orange curve is the best theoretical fit using Eq. (13) where $\tau_g(x_0) = 0$.

The maximum value of the measured contrast is equal to 95%, due to a slight photometric imbalance between the two interferometric arms, differences between the PPLN spectral responses and polarization control defect. Moreover, non-zero values of the contrast when the two fringe patterns are 180° phase shifted can be attributed to a photometric imbalance between them.

5. Conclusion

In this paper, we have described a new experimental method to control the spectral phase in a SFG interferometer analyzing a broadband infrared source. In a proof-of-principle experiment, this novel method was implemented on a SFG interferometer powered by two independent pumps. After cancellation of the differential group delay, the fringe contrast has been maximized by only acting on the pump differential phase. This experimental dual line configuration could be extended to a set of pump lines as long as the differential phase curvature remains negligible over the related spectral bandwidth.

This first demonstration has been achieved taking care to passively reduce, in laboratory, the global optical path fluctuation. For a future on-site implementation, this method could allow developing an active servo control configuration to stabilize an interferometer perturbed by a more stringent thermal and vibrational environment.

We note that, without adding any new component, the same experimental setup can be operated in a spectroscopic mode. The phase modulators on the pump paths would be driven with a temporal optical path modulation instead of the steady voltage offset to create a differential spectral phase function as a function of time. This temporal modulation would allow us to display the power spectral density of the different fringe systems through a Fourier transform in the same way as for Fourier spectroscopy.

Funding

Centre National d'Études Spatiales (CNES) (DCT/SI/OP/2014-8011); Thales Alenia Space (PhD fundings); Institut National des Sciences de l'Univers (INSU) (AO2016–986842).

Optics EXPRESS

Acknowledgments

This work is supported by the Centre National d'Études Spatiales (CNES), Thales Alenia Space and the Institut National des Sciences de l'Univers (INSU). We would like to acknowledge Alain Dexet for his advice and the realization of the mechanical parts.